ASTROMETRIC AND PHOTOMETRIC STUDIES FOR SOME SELECTED OPEN STAR CLUSTERS

R.M.HARIRY[1], A.A.HAROON[1,2], A.A.MALAWI[1]

In this study, we conducted a detailed astrometric, and photometric study of four open clusters (SAI 43, SAI 47, SAI 63, and SAI 113) using data from Gaia DR3. The ASteCA code enabled the identification of the astrometric and photometric parameters. The new centers of these clusters were redetermined and from Radial Density Profile (RDP), the cluster radii, are between 3.13- and 6.6 arcmin for all clusters. The astrophysical parameters are as follows: the number of star members N are 141 (SAI 43), 153 (SAI 47), 198 (SAI 63), and 188 (SAI 113); parallax (ϖ) for SAI 43, SAI 47, SAI 63, and SAI 113 are between 0.275 and 0.506 mas; proper motion parameters ($\mu_a \cos\delta$, μ_δ) are (0.57, -0.54 mas/yr), (0, -0.34 mas/yr), (-0.24, 0.26 mas/yr), and (-5.61, 2.84 mas/yr) for SAI 43, SAI 47, SAI 63, and SAI 113, respectively. The photometric parameters include the color magnitude diagram (CMD), ages, reddening, and distances. The ages are provided as log (age), and they are between (7.172-8.659); the color excess E(B-V) is 0.476±0.017 mag for SAI 43, 0.375±0.014 mag for SAI 47, 0.510±0.009 mag for SAI 63, and 1.265±0.011 mag for SAI 113, the distance modules of the clusters are between 11.177-13.439 mag, and the distances from the sun to each of the clusters (SAI 43, SAI 47, SAI 63, and SAI 113) are calculated as 4900±100 pc, 2360±30 pc, 1720±20 pc, and 3720±50 pc, respectively.

Keywords: *open clusters: astrometric: ASteCA code: database: Gaia DR3: photometric: color magnitude diagram*

1. *Introduction*. Open clusters (OCs) are celestial objects that form within giant molecular clouds (GMCs) that are located in the Milky Way Galaxy disk [1,2]. OCs enable the understanding of star formation, galactic structure, stellar dynamics, and stellar evolution. OCs are young and bright and located in the Galactic plane; thus, they are easy to observe and study [3]. They are excellent laboratories for studying stellar physical and dynamic evolution; therefore, they are easily used to explore the history of star formation and the mechanisms of its formation [4-7]. We used the selected open star cluster data from the European Space Agency's Gaia Data Release 3 (DR3) [8]. The collaboration of the Gaia mission released the DR3, which provides the following astrometric parameters: Galactic position (*l*, *b*), ($\mu_a \cos\delta$, μ_δ), (ϖ), and the radial density profile (RDP). The photometric parameters include a color magnitude diagram (CMD) with the use of three filters (G, blue G_BP, and red G_RP photometric magnitude) for approximately 1.8 billion sources with a brightness greater than 21 mag. Gaia DR3

has complemented and provided more accurate data than previous data sources, such as Gaia DR2 for cluster SAI 43 and 2MASS for clusters SAI 47, SAI 63, and SAI 113. In this study, a wide characterization of these clusters is provided with the aid of the Automated Stellar Cluster Analysis (ASteCA)[1] code [9].

From previously studies, we extracted the astrometric and photometric parameter data for the clusters. Based on the study by [10], the cluster SAI 43 has 135 stars, the proper motion is 0.611 mas/yr in the right ascension (RA), and the proper motion is 0.555 mas/yr in the declination (Dec.). Similarly, for SAI 43, the parallax is 0.109 mas, log(age/year) is 8.410, the cluster is 4451 pc from the Sun, the cluster has a metallicity [Fe/H] -0.198 dex, and its color excess is 1.538 mag. Based on [11], for cluster SAI 47, proper motion is -0.03 ± 1.97 mas/yr in right ascension, the proper motion is 2.55 ± 1.97 mas/yr in declination, the log(age/year) is (8.60 ± 0.05), the cluster is at a distance of 3680 ± 70 pc from the Sun, and color excess is 0.42 mag. From [12], cluster SAI 63 has 142 stars, the cluster's age is 450 ± 50 Myr, the cluster is at a distance of 2.2 ± 0.2 kpc from the Sun, its extinction is 0.44 ± 0.05 mag, and its galactocentric is 10.5 kpc. From [13], SAI 113 has log (age/year) of 7.11, with distance 3.90 ± 0.19 kpc from the Sun, variable reddening from 0.84 to 1.29 mag, and distance modules of 12.95 mag.

The article is structured as follows: Section 2 presents the Gaia DR3 data and the methods used in this study. Section 3 provides the results from the DR3 data analysis for the open clusters, and the astrometric, and photometric parameters are derived. Finally, Section 4 summarizes our conclusions.

2. *Gaia DR3 data and analysis tools*. In this research, we use Gaia DR3 data for the membership determination. These data provide the astrometric parameters (α, δ, l, b, μ, and ϖ), and photometric magnitudes (G, G_BP, and G_RP) for the clusters with their uncertainties. We obtain the astrometric and photometric data of the four clusters from the SAI Open Clusters Catalog[2] ([14]), review previously published research, and download the four clusters' new data sheets from the online catalog VizieR[3], which contains 168 star cluster candidates; these candidates were identified and listed by [15]. We select the OC spatial coordinates with a hypothetical radius equal to 20 arcmin; this value is greater than the cluster radius r_{cl} determined from previous work [14].

Fig.1 shows the open cluster information with the following data: for SAI 43 with $G \leq 20.98$ mag, the average photometric error is 0.004 mag of the *G* magnitude, with a maximum error of 0.0203 mag, and the average photometric error in the *BP - RP* color index is 0.076 mag, with a maximum error of 0.619

THE ADOPTED COORDINATES OF THE CLUSTERS, BOTH EQUATORIAL (α, δ) AND GALACTIC (l, b) SYSTEMS, WERE TAKEN FROM THE SAI OPEN CLUSTER CATALOG

Cluster	Equatorial coordinates		Galactic coordinates	
	α (hh:mm:ss)	δ (dd:mm:ss)	l (deg)	b (deg)
SAI 43	05:08:16.600	49:52:08.000	158.608	5.685
SAI 47	05:23:58.000	42:18:52.000	166.370	3.546
SAI 63	06:13:44.500	06:56:58.000	202.415	-5.134
SAI 113	10:22:43.600	-59:30:20.000	285.064	-1.895

mag; for SAI 47 with $G \leq 20.92$ mag, the average photometric error is 0.004 mag of the G magnitude, with a maximum error of 0.0259 mag, and the average photometric error of the BP-RP color index is 0.060, with a maximum error of 1.741 mag; for SAI 63 with $G \leq 20.86$ mag, the average photometric error is 0.0054 mag of the G magnitude, with a maximum error of 0.055 mag, and the average photometric error of the BP-RP color index is 0.095 mag, with a maximum error of 0.898 mag; and for SAI 113 with, $G \leq 21.14$ mag, the average photometric error is 0.005 mag in the G magnitude, with a maximum error of 0.038 mag, and the average photometric error of the BP-RP color index is 0.103 mag, with a maximum error of 3.266 mag.

In this study, we aim to provide a comprehensive description of the four OCs using a program for this purpose. The ASteCA code is designed with many functions that use position and photometric data. It is available online with full documentation. The code automatically computes the astrometric and photometric parameters of OCs. This code is integrated with the Bayesian field star decontamination algorithm to assign membership probabilities from the theoretical isochrones to select the best fit through a genetic algorithm. The isochrone fitting process allows ASteCA to provide particular estimates for a cluster's parameters, age, metallicity, extinction, and distance values with their uncertainties. Perren et al. [9] provided a full description of the code on the code's website.

3. *Results and discussion*.

3.1. *Astrometric structural analysis*. In cluster analysis, the membership of stars in cluster regions is important to assess. The stars of the open cluster regions are gravitationally bound together, and their proper motions are distributed tightly around the mean proper motion value, which is very useful in membership determination [16,10].
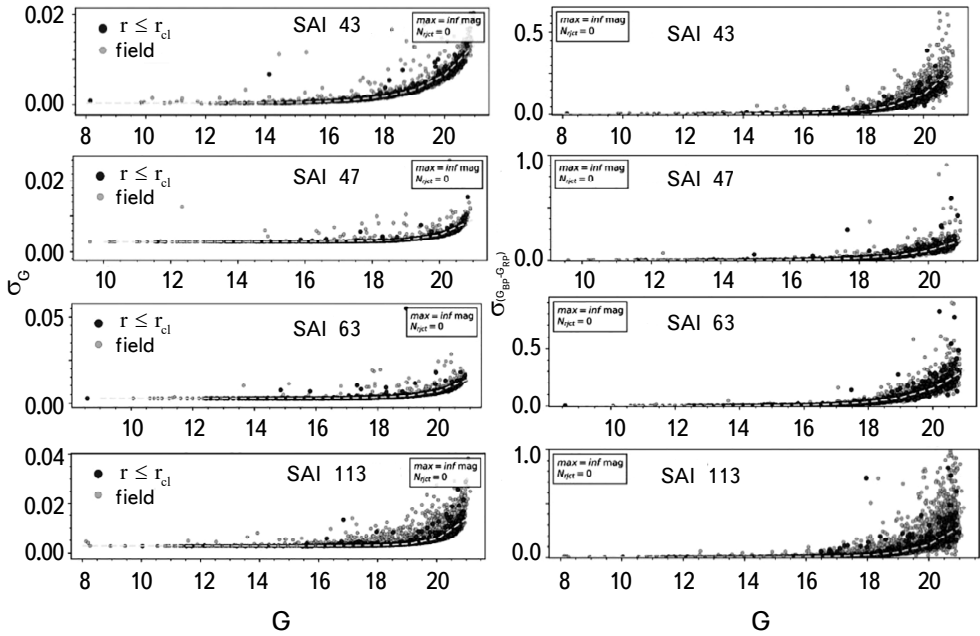
Fig.1. Uncertainties in the photometric magnitude bands; σ_G and σ_{BP-RP} in SAI 43, SAI 47, SAI 63, and SAI 113.

3.1.1. *Re-determination of the cluster's centers*. By recalculating the cluster center (Table 1) using ASteCA, the cluster is taken at the highest stellar density of the cluster region, as shown in Fig.2. and the stars in each bin are counted for both directions. Table 2 lists the coordinates of the estimated new center of the clusters. The new centers of the clusters are in good agreement with the results from the SAI Open cluster catalog, with minimal changes in both the RA and Dec. directions ($\Delta\alpha \leq 1''.997$, $\Delta\delta \leq 19''.22$). The new estimated centers of the clusters SAI 43, SAI 47, SAI 63, and SAI 113 are listed in Table 2.

Table 2

THE COORDINATES OF OUR ESTIMATED NEW CENTER
POSITIONS OF THE CLUSTERS

Cluster	Equatorial coordinates		Galactic coordinates	
	α hh:mm:ss	δ dd:mm:ss	l deg	b deg
SAI 43	05:08:17.510	49:51:48.780	158.614	5.684
SAI 47	05:23:58.690	42:18:49.400	166.372	3.547
SAI 63	06:13:46.497	06:56:47.000	202.755	-4.545
SAI 113	10:22:43.788	-59:30:16.063	285.391	-1.988
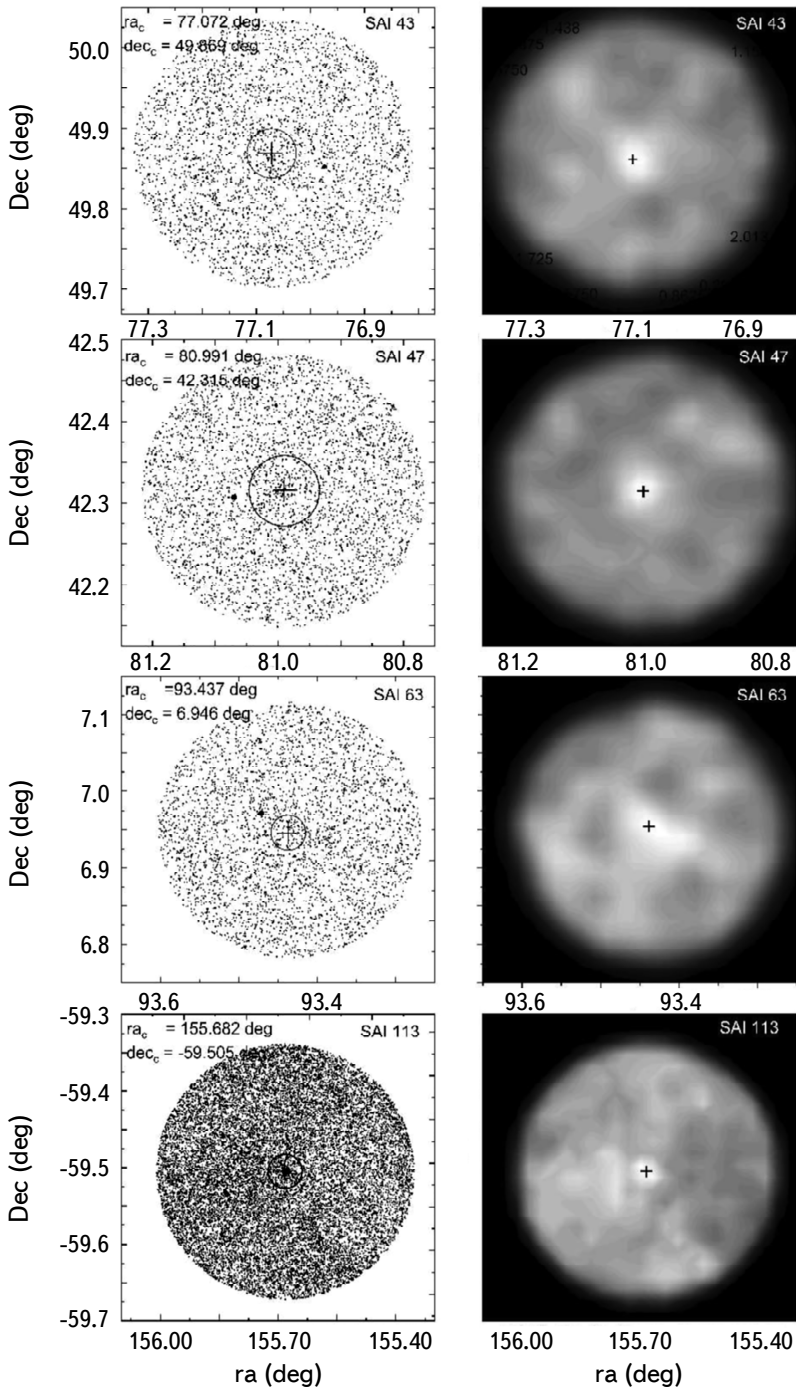
Fig.2. Structural analysis of clusters SAI 43, SAI 47, SAI 63, and SAI 113 acquired by ASteCA. Left panel: analyzed frame with the estimated cluster region with a black circle at the center of the frame and the center of the clusters marked with black + sign. Right panel: 2D density contour map of the same frame.

3.1.2. *Radial density profile (RDP)*. The radial density profile is the density ρ of the number of stars N per zone area along the cluster radius. The surface density distribution $\phi(R)$ of the King's [17] model is expressed as a function of tidal radius r_t and core radius r_c, is:

$$\phi(R) = k \left[\left(1 + (r/r_c)^2\right)^{-1/2} - \left(1 + (r_l/r_c)^2\right)^{-1/2} \right]^2 , \tag{1}$$

where k is a constant. By determination the density function $\rho(r)$ in concentric rings as a function of the radius r from the cluster center outward. To achieve this, we utilize the King's model [18], which is an approximation of King's formula as represented by Equation (2):

$$\rho(r) = \rho_{bg} + \frac{\rho_0}{1 + (r/r_c)^2} , \tag{2}$$

where ρ_{bg} and ρ_0 are the background and central surface density, respectively. r_c is the core radius and is the distance at which the stellar density equals half the central density. Using the ASteCA code, we generated RDP fitting for four clusters (SAI 43, SAI 47, SAI 63, and SAI 113), and each cluster was fit with a King profile, as shown in Equation (2) [17,18]. As shown in Fig.3, a peak is observed in the density distribution near the cluster center; this peak decreases and flattens after a certain point and shows the cluster density of the field stars. At that value, we can estimate the cluster radius or limiting radius, r_{cl}, which covers the entire cluster area and at which the line represents the value of the background density (dashed black horizontal lines in the figure) that intersects with the King profile fitting curve.

After we applied the RDP fitting, we estimated the internal cluster structural parameters for the clusters; these include r_c, r_{cl}, tidal radius r_t, ρ_0, and ρ_{bg}. The values of the core radius and the tidal radius are given by ASteCA code with their upper and lower values estimates as shown in Fig.3.

The point of ρ_{bg} is given by ($\rho_{bg} + 3\sigma_{bg}$), where σ_{bg} is the uncertainty of ρ_{bg}. Bukowiecki et al. [19] derived the following expression for the limiting radius:

$$r_{cl} = r_c \sqrt{\frac{\rho_0}{3\sigma_{bg}} - 1} , \tag{3}$$

where all radii are measured in arcminutes (arcmin), while all densities are measured in stars/arcmin^2. By fitting the King model to the RDP, the estimated r_{cl} was obtained by using Equation (3). Moreover, the ASteCA represents the value of r_t for an open cluster; here, r_t is the radial distance from the cluster center at which the gravitational acceleration produced by the cluster is approximately equal to the tidal acceleration produced by the Galaxy [20]. Certain parameters are used to characterize the structure of open clusters. One of these parameters

is the density contrast parameter δ_c, which is the stellar density contrast of the clusters against the background population; this parameter measures the compactness of a cluster [21] and is calculated using the following equation:

$$\delta_c = 1 + \frac{\rho_0}{\rho_{bg}}.$$

(4)

Another parameter is the concentration parameter C, which is the log ratio of the cluster r_t to its r_c [22]. C can be calculated using the following equation:

$$C = \log\left(\frac{r_t}{r_c}\right).$$

(5)

All numerical parameter results are listed in Table 3.

OBTAINED STRUCTURAL PROPERTIES FOR THE FOUR OCs
AS COMPUTED FROM THE RDP FITTED BY KING's DENSITY
PROFILE USING ASteCA CODE

Parameters	SAI 43	SAI 47	SAI 63	SAI 113
r_{cl} (arcmin)	3.58	3.13	5.40	6.60
r_c (arcmin)	$2.02^{2.97}_{1.17}$	$1.38^{2.08}_{0.73}$	$3.78^{5.19}_{2.41}$	$2.64^{3.80}_{1.41}$
r_t (arcmin)	$5.04^{6.36}_{3.88}$	$5.20^{6.00}_{4.37}$	$8.90^{10.30}_{7.42}$	$11.82^{12.86}_{10.75}$
ρ_0 (stars arcmin^{-2})	15.02	25.57	16.63	43.22
ρ_{bg} (stars arcmin^{-2})	6.54	9.57	11.12	29.52
δ_c	3.30	3.67	2.41	2.46
C	0.40	0.58	0.37	0.65

It should be noted that the values of the core radius and the tidal radius are with their upper and lower values estimates.

3.1.3. *Astrometric parameters and distance determination*. Astrometric parameters are used to identify the stellar membership of each of the clusters by performing a membership analysis using proper motion and parallax; these are important astrometric parameters for this mission, and data from the Gaia DR3 database are used to obtain the proper motion and parallax. We acquired a comprehensive data sheet for all stars with a photometric magnitude ($G < 21$ mag). The ASteCA code was utilized to input all the data points and determine the membership probability. This was achieved by identifying a significant stellar over density and comparing it to the surrounding stellar field.

Also, ASteCA utilizes a Bayesian field star purification method that allocates membership probabilities only based on photometric data. A Bayesian decontami-
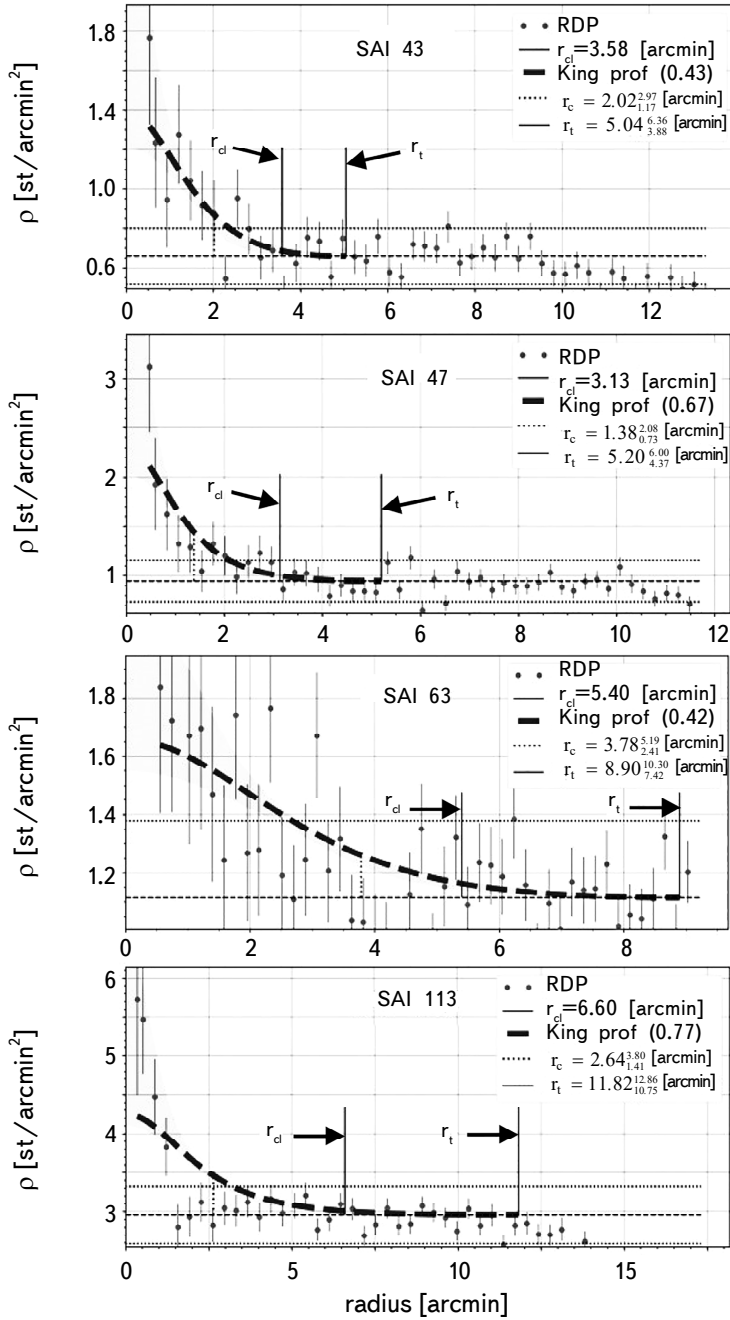
Fig.3. RDP for the four open clusters. The grey dots are the RDP for the four open clusters (SAI 43, SAI 47, SAI 63, and SAI 113) obtained with the aid of the ASteCA code. The thick black dashed line and shaded area represent the King's density profile. The black dashed lines denote the background field density ρ_{bg} . The black dotted lines denote the central surface density ρ_0 . The Vertical lines indicate the structural parameters: grey line r_{cl}, grey dotted horizontal line r_c, and grey line r_t of each cluster. The small numbers above and below the value of r_c, and r_t represent the range of these parameters.

nation algorithm (DA) was created using a nonparametric probability model-based technique that follows an iterative procedure inside a Bayesian framework. The code includes functions for structural analysis, statistically improved color estimations free of field star contamination [9]. Our results show that the number of these most probable members with membership probability $P \geq 50\%$ for the clusters are 141 for SAI 43, 153 for SAI 47, 198 for SAI 63, and 257 for SAI 113. These members lie within the cluster diameter and are located in the ranging parallax and proper motion errors in the RA and Dec.

We plotted the stellar distribution for the cluster members and background stars' proper motion ($\mu_a \cos\delta$, μ_δ) for the clusters, as shown in the upper panel of Fig.4. The mean proper motion for each cluster is determined by applying Gaussian fitting for the cluster directions, as shown in the lower panel of Fig.4, the average PM outputs ($\mu_a \cos\delta$, μ_δ) are (0.57, -0.54), (0, -0.34), (-0.24, 0.26), and (-5.61, 2.84) for SAI 43, SAI 47, SAI 63, and SAI 113, respectively.

In Fig.5 we show the Bayesian parallax analysis proposed by [23] on the cluster region stars. This analysis makes use of all stars, even those with negative parallax values of no apparent (physical) value. The distances obtained are heavily affected by the selected offset applied on the parallax.
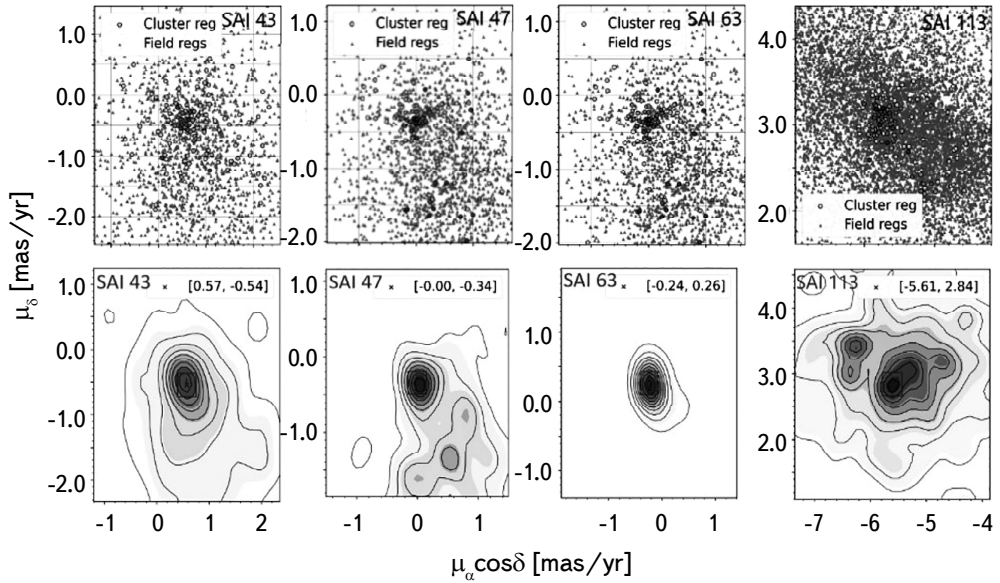
Fig.4. Proper motion, contour map of proper motion. Upper panel: Stellar distribution of the cluster members, and field stars' proper motion (μ; mas/yr) in both directions of right ascension and declination, and it appears that the cluster members are clearly very much embedded within the field stars' distribution. Lower panel: contour map of stellar distribution of the proper motion (μ; mas/yr) in both directions of right ascension and declination show the value of proper motions for the four clusters.
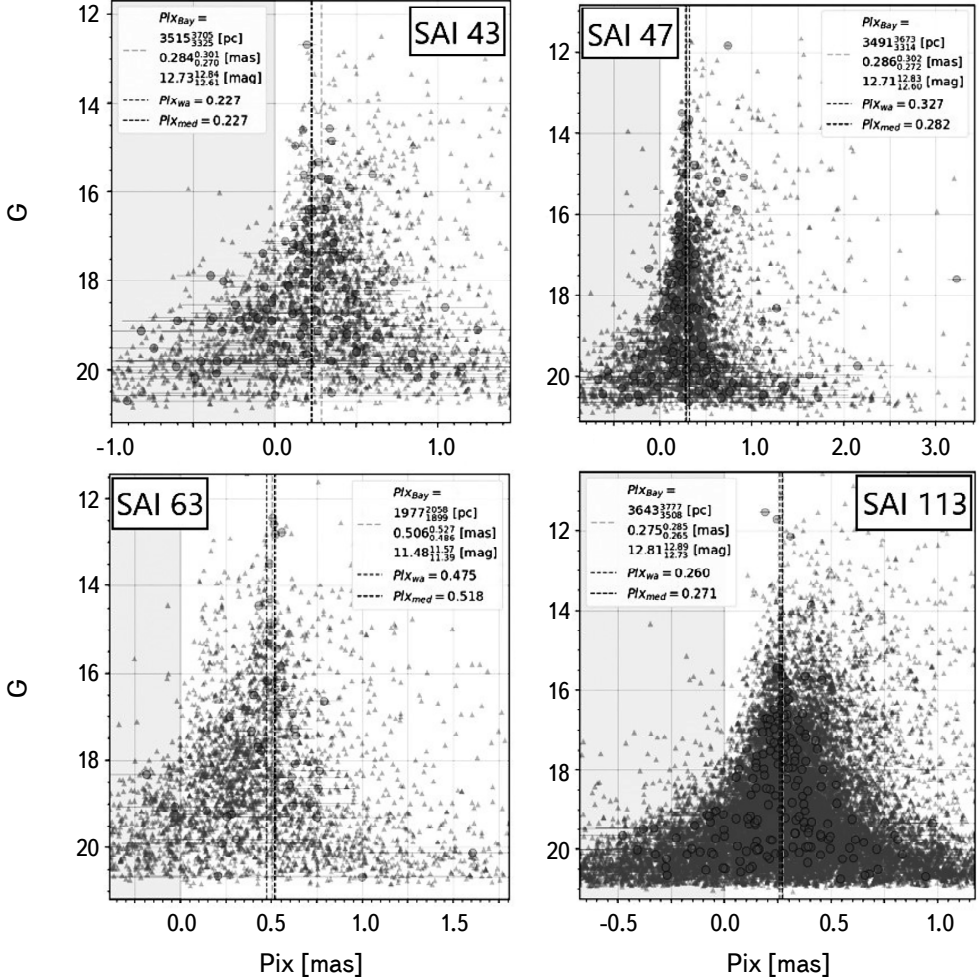
Fig.5. Parallax distribution for all stellar member candidates in the cluster space with gray circle has horizontal line, the triangle for field stars, the vertical grey dashed line plxBay, ASteCA parallax plxmed with the black dotted line and the weighted average with the medium grey dashed line plxwa, where the weights are the inverse of the parallax errors.

We applied the Bayesian distance d_{Bayes} found by the code depend on [23] is shown in Fig.5. This shows a plx_{Bay} vertical grey dashed line, ASteCA distance d_{ASteCA} with the black dotted line from plx_{med} and the weighted average with the light grey dashed line from plx_{wa} (where the weights are the inverse of the parallax errors). From Fig.5, we found Bayesian parallax of the four open cluster members: $0.284_{0.270}^{0.301}$ for SAI 43, $0.286_{0.272}^{0.302}$ for SAI 47, $0.506_{0.486}^{0.527}$ for SAI 63, and $0.275_{0.265}^{0.285}$ for SAI 113. After obtaining the values of the clusters' parallax uses these values to calculate the distance for each cluster based on its parallax [24]. The astrometric distances calculated for SAI 43, SAI 47, SAI 63, and SAI 113 are as follows:
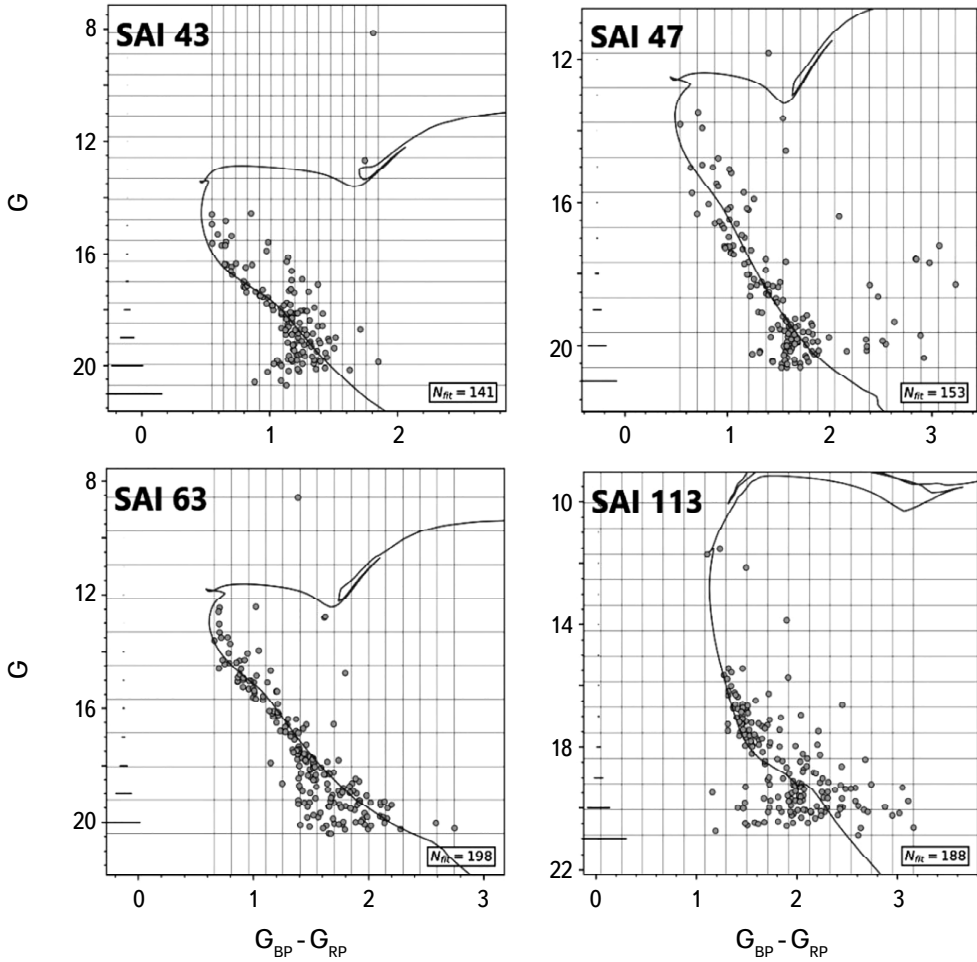
Fig.6. CMDs for the star members of open clusters SAI 43, SAI 47, SAI 63, and SAI 113. The graphs demonstrate the relationship between G and (G_BP-G_RP). The data (the grey dots) are adjusted using the extinction isochrone corrected by [24], which is represented by the black curved lines.

3515^{3705}_{3325}, 3491^{3673}_{3314}, 1977^{2058}_{1899}, and 3643^{3777}_{3508}, respectively. The small numbers above and below the parallax value, and above and below the distance value represents the range of these values.

3.2. *Photometric analysis: Color magnitude diagram (CMD)*. We use ASteCA to estimate the photometric values (reddening, metallicity, age, and distance) of the final memberships of the clusters. ASteCA includes isochrones and the best fitting operations that generate artificial CMDs of the clusters from the isochrones and the best fit of the genetic algorithm. Using the isochrones of the specific metallicity Z and age log(age/yr) selected from the CMD v3.6 service,

we drew the corresponding CMD using DR3 photometric magnitudes (G, G_BP, G_RP) for the stars (Fig.6). By using ASteCA, the PARSEC v1.2S [25] theoretical isochrones[4] for Gaia DR3 [26] were applied to estimate the cluster metallicity and age.

The photometrical distances d_{phot} estimated from CMD to the cluster (in pc) are 4900 ± 100, 2360 ± 30, 1720 ± 20, and 3720 ± 50 for clusters SAI 43, SAI 47, SAI 63, and SAI 113, respectively.

All these astrophysical and photometric parameters are listed in Table 4. The reddening parameter E(G_BP - G_RP) and E(B - V) colour excess based on data obtained from Gaia photometry are determined from the color band by using the following formula [26]:

$$E(G\_BP - G\_RP) = 1.289\, E(B - V). \qquad (6)$$

Also, formula (6) were used to estimate the reddening.

Table 4

THE CALCULATED ASTROPHYSICAL AND PHOTOMETRIC
PARAMETERS OF THE FOUR OPEN CLUSTERS, WITH A
COMPARISON FROM THE DATA TAKEN FROM THE SAI
OPEN CLUSTERS CATALOG

Parameters	SAI 43	SAI 47	SAI 63	SAI 113	Ref.
Number of Members	141	153	198	188	Our work
$\mu_a \cos\delta$ (mas/yr)	0.57	0	-0.24	-5.61	Our work
μ_a (mas/yr)	-0.54	-0.34	0.26	2.84	Our work
ϖ (mas)	$0.284_{0.270}^{0.301}$	$0.286_{0.272}^{0.302}$	$0.506_{0.486}^{0.527}$	$0.275_{0.265}^{0.285}$	Our work
d_{plx} (pc)	3515_{3325}^{3705}	3491_{3314}^{3673}	1977_{1899}^{2058}	3643_{3508}^{3777}	Our work
Z	0.0146±0.001	0.029±0.0002	0.0192±0.0002	0.009±0.0003	Our work
log (age/yr)	8.407±0.032	8.634±0.004	8.659±0.012	7.172±0.024	Our work
	8.95±0.050	8.5±0.050	8.65±0.050		[14]
$E(B - V)$ (mag)	0.476±0.017	0.375±0.014	0.510±0.009	1.265±0.011	Our work
	0.18±0.03	0.6±0.01	0.37±0.13		[14]
E(G_BP-G_RP) (mag)	0.61±0.02	0.48±0.02	0.66±0.01	1.63±0.01	Our work
A_G (mag)	1.15±0.04	0.91±0.04	1.25±0.02	3.08±0.03	Our work
$(m - M)_0$ (mag)	13.43±0.05	12.267±0.034	11.177±0.020	12.853±0.031	Our work
	12.92±0.07	12.93±0.05	11.4±0.09		[14]
d_{phot} (pc)	4900±100	2360±30	1720±20	3720±50	Our work
	3840±130	3860±90	1910±80		[14]
R_{gc} (kpc)	9.0±0.1	6.1±0.1	8.2±0.1	6.9±0.1	Our work
$X_\odot$ (kpc)	-1.34±0.03	1.30±0.02	0.03±0.0004	1.32±0.02	Our work
$Y_\odot$ (kpc)	4.70±0.01	0.26±0.003	-0.28±0.003	1.34±0.03	Our work
$Z_\odot$ (kpc)	-0.29±0.006	-1.95±0.02	1.70±0.02	-3.40±0.05	Our work

---

[4] *http://stev.oapd.inaf.it/cgi-bin/cmd.*

Reddening with a line-of-sight absorption coefficient A_G computed by [27] and [28] is used to correct the observed data:

$$A_G = (1.890 \pm 0.015) E(G\_BP - G\_RP). \tag{7}$$

The results after using Equations (6) and (7) are recorded in Table 4. The distance to the Galactic center R_{gc} for the clusters is calculated using the estimated photometric distances to these cluster Equation (8):

$$R_{gc} = \sqrt{R_0^2 + (d \cos b)^2 - 2 R_0 d \cos b \cos l}, \tag{8}$$

where $R_0 = 8.20 \pm 0.10 \, \text{kpc}$ [29]. The expected distance toward the Galactic plane ($X_\odot$, $Y_\odot$) and the distance above the Galactic plane ($Z_\odot$) can be computed by using the following relation [30]:

$$X_\odot = d \cos b \cos l, \quad Y_\odot = d \cos b \sin l, \quad Z_\odot = \sin b, \tag{9}$$

where ($X_\odot$, $Y_\odot$, and $Z_\odot$) are the heliocentric Cartesian coordinates of the clusters. All results from the astrophysical and photometric parameters are listed in Table 4.

4. *Conclusion*. In this study, we present an astrometric and photometric study of open clusters SAI 43, SAI 47, SAI 63, and SAI 113 using data from Gaia DR3 with the aid of the ASteCA code.

The astrometric parameters, such as cluster position, cluster radius, core radius, tidal radius, proper motion, parallax, and distance, are determined. Photometric parameters such as metallicity, age, total-to-selective extinction, reddening, and distance modulus are measured after estimating their members. All calculations and estimates of the clusters are used to understand the evolution of these clusters. The main results of the present study are as follows:

1. We used the ASteCA code for each cluster to estimate the clusters astrometric parameters such as mean proper motion, parallax, and RDP to determine the limiting radius, after utilizing membership probabilities $P \geq 50\%$, which identified the most probable member stars for the individual clusters (141; SAI 43, 153; SAI 47, 198; SAI 63, and 188; SAI 113) lying in the mean proper motion.

2. We redetermined the new cluster position by using the ASteCA code; our results were in agreement with those estimated from the SAI Catalog with minimal changes in both the RA and Dec. directions ($\Delta\alpha \leq 1''.997$, $\Delta\delta \leq 19''.22$).

3. After correction for systematic error for parallax by adding $+0.021 \, \text{mas}$, we calculated the astrometric distances from parallax for SAI 43, SAI 47, SAI 63, and SAI 113 are as follows: 3515_{3325}^{3705}, 3491_{3314}^{3673}, 1977_{1899}^{2058}, and 3643_{3508}^{3777}, respectively.

4. The photometric parameters were also determined by the ASteCA code. By applying [23] Bressan et al. theoretical isochrones of metallicity Z to fit to the CMD of most probable cluster members with the best fit values. The clusters age

(in a log scale), reddening, and distance modules $(m\text{-}M)_0$ were determined. By using the distance modules values to calculate the photometric distance of the clusters d_{phot} we get: 4900 ± 100 pc for SAI 43, 2360 ± 30 pc for SAI 47, 1720 ± 20 pc for SAI 63, and 3720 ± 50 pc for SAI 113. The distances of the clusters from the galactic plane, $Z_\odot$, as well as their projected distances from the Sun, $X_\odot$, and $Y_\odot$, and the galactic centers R_{gc}, were then calculated and are all shown in Table 4.

[1] Astronomy and Space Science Department, Faculty of Science, King Abdul Aziz University, Saudi Arabia, e-mail: rhariry@hotmail.com
[2] Astronomy Department, National Research Institute of Astronomy and Geophysics (NRIAG), Cairo, Egypt

АСТРОНОМИЧЕСКИЕ И ФОТОМЕТРИЧЕСКИЕ ИССЛЕДОВАНИЯ НЕКОТОРЫХ ВЫБРАННЫХ РАССЕЯННЫХ ЗВЕЗДНЫХ СКОПЛЕНИЙ

Р.М.ХАРИРИ[1], А.А.ХАРУН[1,2], А.А.МАЛАВИ[1]

В данном исследовании выполнен детальный астрометрический и фото-метрический анализ четырех рассеянных звездных скоплений (SAI 43, SAI 47, SAI 63 и SAI 113) с использованием данных Gaia DR3. Код ASteCA был применен для определения астрометрических и фотометрических параметров. Заново определены центры этих скоплений. Радиусы скоплений, определенные на основе радиального профиля плотности (RDP), варьируются в пределах 3.13-6.6 угловых минут для всех скоплений. Астрофизические параметры скоплений следующие: число членов (N) составляет 141 (SAI 43), 153 (SAI 47), 198 (SAI 63) и 188 (SAI 113); параллаксы (π) для SAI 43, SAI 47, SAI 63 и SAI 113 находятся в диапазоне от 0.275 до 0.506 mas; параметры собст-венного движения ($\mu_a\cos\delta$, μ_δ) равны (0.57, -0.54 mas/yr), (0, -0.34 mas/yr),

(-0.24, 0.26 mas/yr) и (-5.61, 2.84 mas/yr) для SAI 43, SAI 47, SAI 63 и SAI 113, соответственно. Фотометрические параметры включают диаграмму цвет-звездная величина (CMD), возраст, поглощение света и расстояния. Возраст представлен как log(age) и варьируется в пределах 7.172 - 8.659. Избыток цвета E(B - V) составляет 0.476 ± 0.017 зв. вел. для SAI 43, 0.375 ± 0.014 для SAI 47, 0.510 ± 0.009 для SAI 63 и 1.265 ± 0.011 для SAI 113. Модули расстояний для скоплений находятся в диапазоне 11.177 - 13.439 зв. вел., а расстояния от Солнца до каждого из скоплений (SAI 43, SAI 47, SAI 63 и SAI 113) рассчитаны как 4900 ± 100 пк, 2360 ± 30 пк, 1720 ± 20 пк и 3720 ± 50 пк, соответственно.

REFERENCES

1. *C.J.Lada*, *E.A.Lada*, Ann. Rev. Astron. Astrophys., **41**, 57, 2003.
2. *S.P.Zwart*, *S.L.W.McMillan*, *M.Gieles*, Ann. Rev. Astron. Astrophys., **48**, 431, 2010.
3. *E.M.Ghosh*, *P.Tucio*, *M.Fajrin et al.*, in Journal of Physics: Conference Series, **2214**, no. 1. IOP Publishing, 2022, p.012009.
4. *D.A.VandenBerg*, Astrophys. J. Suppl. Ser., **51**, 29, 1983.
5. *A.Barnes*, Astrophys. J., **669**, 1167, 2007.
6. *C.Bertelli Motta*, *M.Salaris*, *A.Pasquali et al.*, Mon. Not. Roy. Astron. Soc., **466**, 2161, 2017.
7. *A.F.Marino*, *A.P.Milone*, *L.Casagrande et al.*, Astrophys. J. Lett., **863**, L33, 2018.
8. *A.Vallenari*, *A.G.Brown*, *T.Prusti et al.*, Astron. Astrophys., **674**, A1, 2023.
9. *G.I.Perren*, *R.A.Vazquez*, *A.E.Piatti*, Astron. Astrophys., **576**, A6, 2015.
10. *H.Monteiro*, *W.Dias*, *A.Moitinho et al.*, Mon. Not. Roy. Astron. Soc., **499**, 1874, 2020.
11. *L.Yalyalieva*, *E.Glushkova*, *A.Dambis*, Open Astron., **25**, 439, 2016.
12. *R.Yadav*, *S.Leonova*, *R.Sagar et al.*, Astrophys. Astron., **35**, 143, 2014.
13. *G.Carraro*, *D.G.Turner*, *D.J.Majaess et al.*, Astron. J., **153**, 156, 2017.
14. *E.Glushkova*, *S.Koposov*, *I.Y.Zolotukhin et al.*, Astron. Lett., **36**, 75, 2010.
15. *L.Liu*, *X.Pang*, Astrophys. J. Suppl. Ser., **245**, 32, 2019.
16. *T.Cantat-Gaudin*, *C.Jordi*, *A.Vallenari et al.*, Astron. Astrophys., **618**, A93, 2018.
17. *I.King*, Astron. J., **67**, 471, 1962.
18. *I.R.King*, Astron. J., **71**, 276, 1966.
19. *J.Bukowiecki*, *G.Maciejewski*, *P.Konorski et al.*, arXiv:1107.5119, 2011.

20. *S. von Hoerner*, Astrophys. J., **125**, 451, 1957.
21. *C.Bonatto*, *E.Bica*, Mon. Not. Roy. Astron. Soc., **397**, 1915, 2009.
22. *C.J.Peterson*, *I.R.King*, Astron. J., **80**, 427, 1975.
23. *C.A.Bailer-Jones*, Publ. Astron. Soc. Pacif., **127**, 994, 2015.
24. *C.Bailer-Jones*, *J.Rybizki*, *M.Fouesneau et al.*, Astron. J., **161**, 147, 2021.
25. *A.Bressan*, *P.Marigo*, *L.Girardi et al.*, Mon. Not. Roy. Astron. Soc., **427**, 127, 2012.
26. *W.Brandner*, *P.Calissendorff*, *T.Kopytova*, Astron. Astrophys., **677**, A162, 2023.
27. *A.Cardelli*, *G.C.Clayton*, *J.S.Mathis*, Astrophys. J., **345**, 245, 1989.
28. *L.Casagrande*, *D.A.VandenBerg*, Mon. Not. Roy. Astron. Soc. Lett., **479**, L102-L107, 2018.
29. *J.Zhong*, *L.Chen*, *M.Kouwenhoven et al.*, Astron. Astrophys., **624**, A34, 2019.
30. *J.Bland-Hawthorn*, *S.Sharma*, *T.Tepper-Garcia et al.*, Mon. Not. Roy. Astron. Soc., **486**, 1167, 2019.